

Propagation of the Fundamental Mode in Curved Graded Index Multimode Fiber and Its Application in Sensor Systems

Denis Donlagić and Brian Culshaw

Abstract—A novel principle of light transmission through very small radius bend in optical fibers is presented. The potential applications of the proposed structure are fiber optic sensors and other fiber optic systems. The design makes use of graded index multimode fiber as transmission medium. However, the feed to the multimode fiber is through a single mode fiber to ensure that only the lowest order spatial mode is launched. Similarly the receiver is also coupled to the sensing element through a single mode fiber. The fundamental mode within graded index multimode fiber proves to be very insensitive to macrobends if bend radius is larger than certain critical value. If bend radius is reduced below critical value the loss increases very rapidly and this allows for construction of relatively sensitive macrobend fiber optic sensor. This work presents a quantitative theoretical model of the proposed structure and a detailed experimental investigation of structure with possibilities for its practical applications.

Index Terms—Bend loss, fiber optics sensors, macrobends, optical fibers.

I. INTRODUCTION

RADIATION loss caused by curvature of dielectric waveguide is very important from the point of view of fiber-optic transmission of optical signals, fiber optic sensors, and integrated optics. The curvature loss has been therefore studied extensively theoretically and experimentally in the past [1]–[7]. In systems where severe waveguide bends are present high NA fibers, modified index profile waveguides [8], etc., have been utilized in order to reduce bend loss. Additionally, the macrobend loss phenomena have been applied to sensor systems with some success [4], however, their application is limited due to the relatively low sensitivity and large dimensions.

Recently, we reported fiber optic microbend sensor structure (called SMS) based on selective launch of the fundamental mode in graded index multimode fiber [9]. In addition to significantly different microbend properties, the proposed structure also exhibits significantly different macrobend effects. Those effects and their applications are considered in this paper in detail.

The actual transmission and/or sensing element of the SMS structure is graded index multimode fiber. However, the feed

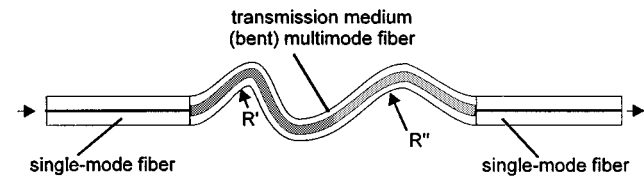


Fig. 1. SMS structure.

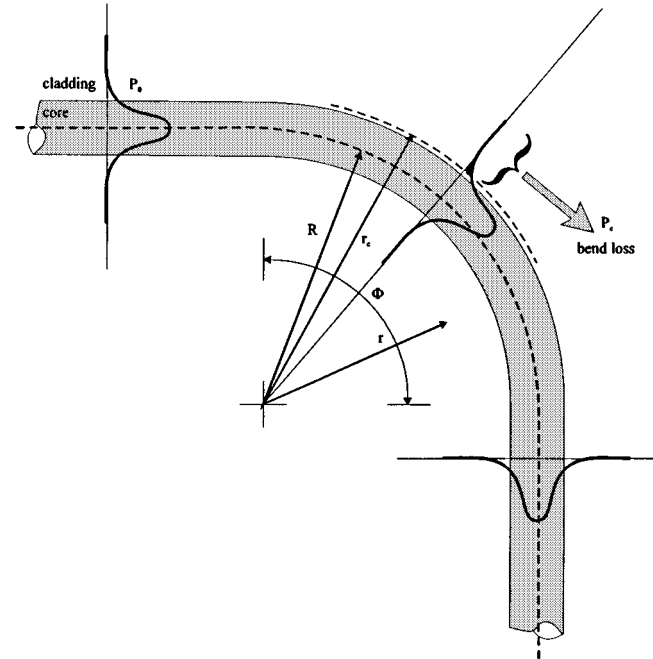


Fig. 2. Macrobend loss in fiber.

to the sensing section is through a single mode fiber spliced to the multimode fiber to ensure that only the lowest order spatial mode is launched. Similarly the receiver is also coupled to the sensing element through a single-mode fiber. The structure is shown in Fig. 1. The overall loss of the structure (single-mode to single-mode transition) is in the range of 1 dB when standard fibers and standard splicing procedure are used and it can be further reduced by optimized fusion splicing down to approximately 0.6 dB (at 1310 nm) for standard fibers [9]. Additionally, the fundamental mode within graded multimode fiber propagates with minimum loss, typically additional loss that results from mode coupling ranges from 0.1 to 0.4 dB/km [9].

Manuscript received July 9, 1999; revised December 1, 1999.

D. Donlagić is with the Faculty of Electrical Engineering and Computer Science, University of Maribor, Maribor 2000, Slovenia.

B. Culshaw is with the Department of Electronic and Electrical Engineering, University of Strathclyde, Glasgow G1 1XW, U.K.

Publisher Item Identifier S 0733-8724(00)02241-6.

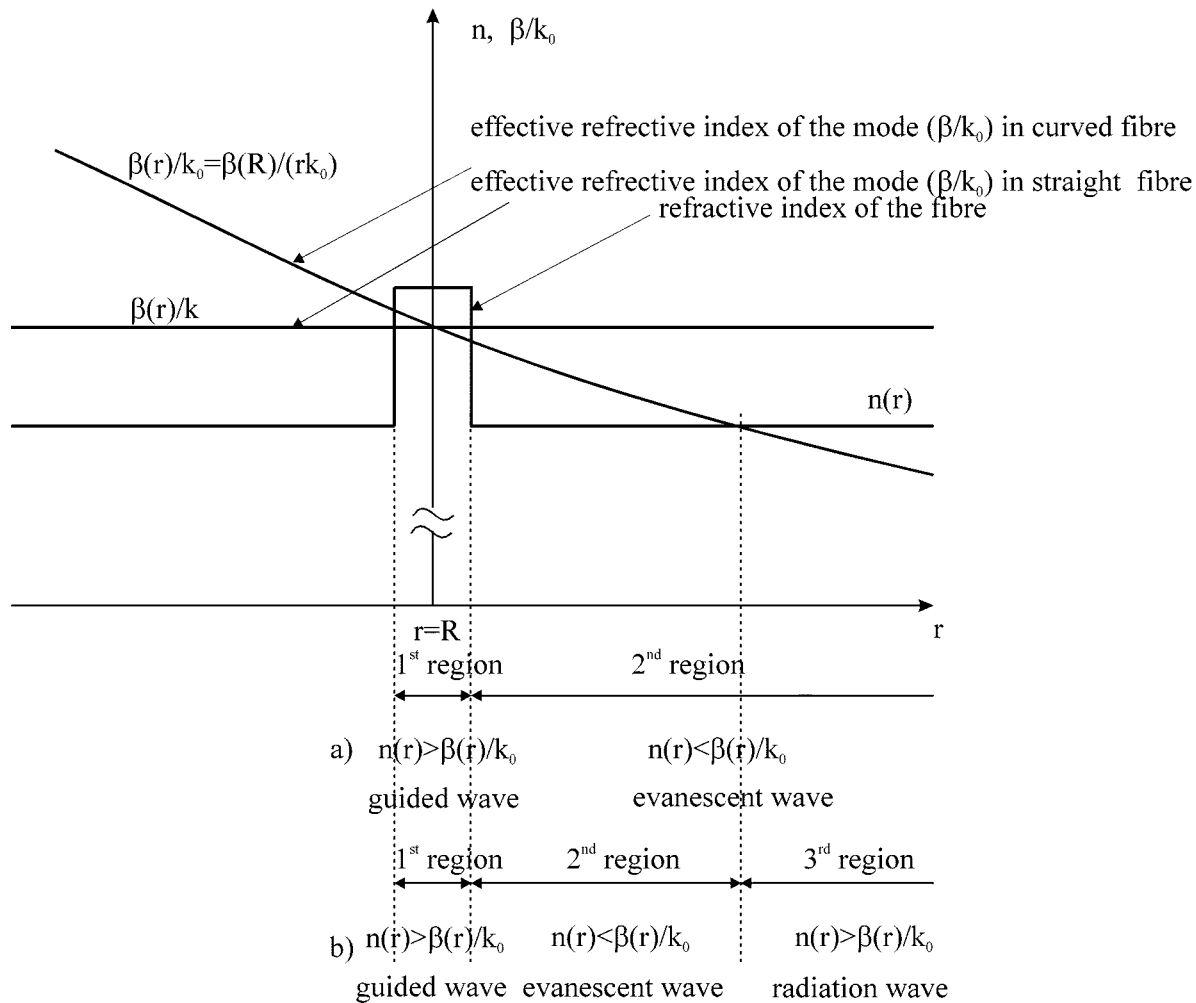


Fig. 3. Straight (a) and bent (b) single-mode step index fiber.

II. THEORY

A. Macrobend Loss: Comparison Between Loss in Single-Mode Fiber and SMS Structure

In the past the bend loss of fundamental mode was studied extensively theoretically [1]–[4] and experimentally [4]–[8] for single-mode step index fibers. Extending those studies to the SMS concept gives quantitative description of macrobend loss in SMS structure.

In single mode fibers the macrobend loss, consists of two components [2], [4], [5]: a transition loss and a pure bend loss.

1) *Transition Loss:* The transition loss in single-mode fiber arises when the mode fields in the straight and the bent fiber segments are not identical. In the bend the central maximum of the mode field is shifted radially outward [2], [4]. At the junction between the straight and bent single-mode fiber segments, a portion of the incident power excites the guided mode in the bent segment and the remaining power is coupled to the continuum of radiation modes.

The transition process in the SMS structure is similar, except that the radial shift of the fundamental mode field is also limited by the graded profile. Additionally, the fraction of power in the bend that does not excite fundamental mode couples to higher order guided modes of the multimode fiber.

2) *Pure Bend Loss:* The pure bend loss results from the continual loss of guiding at the outer portion of the evanescent field of the fundamental mode. This loss of guiding is due to the phase velocity of the outer part of the evanescent field becoming equal to the speed of light in the cladding [3], [4]. The smaller the radius of the bend the greater the fraction of the evanescent field affected and hence greater the percentage of light lost at the bend. The fraction that is affected is the main reason for the differences in macrobend properties of single-mode, multimode, and SMS-based systems.

In the bend region of radius R and angle Φ (Fig. 2), the confining path of fundamental mode is assumed to be circular. In the bend the modal wave front will propagate with a phase velocity linearly dependent on the radial distance from the centre of curvature of the bend. The propagation constant of the mode β , will thus be in proportion to $1/r$

$$\beta(r) = \frac{R}{r} \beta(R). \quad (1)$$

For radial positions larger than a characteristic value r_c , the angular phase velocity of the wave front equals the velocity of light in the propagation medium

$$\frac{\omega}{\beta(r_c)} = \frac{c}{n(r_c)} \Rightarrow \beta(r_c) = n(r_c)k_0 \quad (2)$$

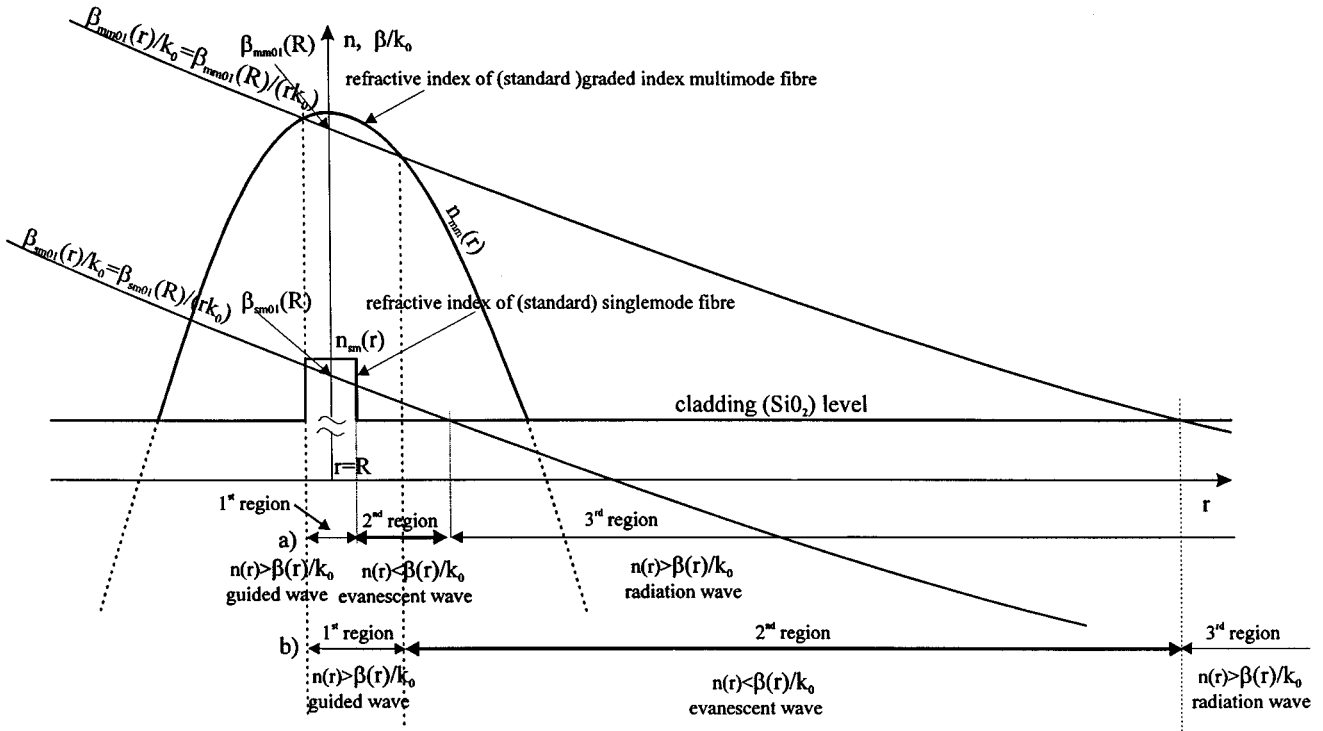


Fig. 4. Bend loss of: (a) fundamental mode launched graded index multimode fiber and (b) single-mode fiber. Fundamental mode of bent graded index fiber has much wider evanescent field as equally bent standard step-index fiber.

and power in the shaded tail P_{loss} dissociates itself from the wave front, propagates in a tangential path to the dissociation point and radiates away [3], [4]. This is obvious when the transversal component k_T of propagation vector is observed:

$$\begin{aligned} k_T(r) &= \sqrt{(k_0 n(r))^2 - \beta^2(r)} \\ &= k_0 \sqrt{n(r)^2 - n_{\text{eff}}(r)^2} \end{aligned} \quad (3)$$

where k_0 is propagation number of optical wave in vacuum, n_{eff} is effective refractive index of the mode.

In bent fiber, one can observe three distinctive regions (Fig. 3).

- First region: region is limited in the transversal plane and k_T is real number ($n(r) > \beta(r)/k_0$): This region represents a guided wave in the core of the fiber.
- Second region: region is limited in the transversal plane and k_T is complex number ($n(r) < \beta(r)/k_0$). This region represents evanescent wave.
- Third region: k_T is again real number ($n(r) > \beta(r)/k_0$), but region is unlimited in the radial direction beyond region 2: this region represents the radiation wave.

In perfectly straight fiber n_{eff} is independent of r , third region disappears and propagation of the wave becomes loss-less. In case of bent fiber, the bend loss depends on the size of evanescent region.

B. Comparison of Pure Bend Loss of Fundamental Mode in Single-Mode and Graded Index Multimode Fiber

When the bend radius is large in comparison to the fiber core diameter, the propagation constants at axis of bent fiber can be approximated by propagation constants of the straight fiber

[1], [8]. The propagation constant of fundamental mode in typical telecommunication graded index multimode fiber is close (i.e., somewhat less than) $n_{\text{max}} k_0$ (n_{max} is maximum refractive index of fiber core). For example in case of 50 μm fiber with NA = 0.2 ($\Delta = 0.0135$) and $n_{\text{max}} = 1.475$ the propagation constant β of fundamental mode is about $1.4738 k_0 = 0.9992 n_{\text{max}} k_0$.

Fig. 4 represents graphical comparison between single mode and fundamental mode launched multimode fiber (index profiles of both fibers shown in Fig. 4 are in proportion to standard single-mode and 62.5- μm core diameter multimode fiber). Fig. 4 clearly demonstrates the difference bend loss behavior of singlemode and fundamental mode launched multimode fiber. The propagation constant β_{mm01} of the fundamental mode in graded index fiber is significantly higher than for singlemode fiber (β_{sm01}). The phase constants of fundamental modes in both (equally bent) fibers decrease with the same rate as r increases [see (1)], The evanescent region is much wider for the multimode graded index fiber, e.g., the point in the cladding where k_t becomes real (start of third region) appears significantly further into the cladding than in the case of single-mode fiber. This results in much lower macrobend sensitivity of fundamental mode in graded index multimode fiber.

The conclusion that we reached from Fig. 4 also indicate several additional properties of the fundamental mode launched bent graded index multimode fiber: 1) hypothetical infinite extending parabolic core tends to support loss-less propagation of waves (the third region where k_t becomes real vanishes), 2) in finite core bent fiber the second (evanescent region) increases (bend loss decreases) if core size reduces and/or NA increases, and 3) in strongly bent fiber the second (evanescent) region

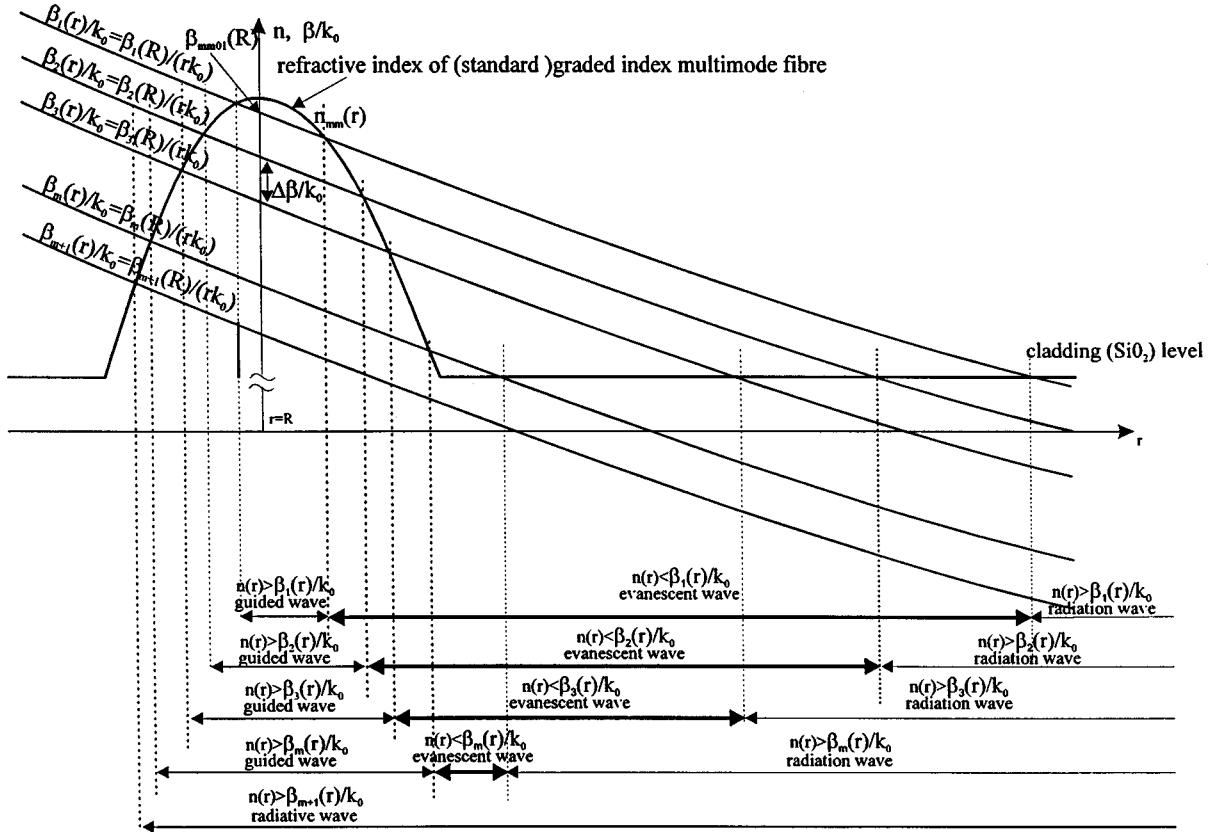


Fig. 5. Higher order modes and bend loss in graded index multimode fiber.

shrinks rapidly at both sides when the radius R decreases, (i.e., this results in a more abrupt change of bend loss below a critical bend radius).

C. Bend Loss of Graded Index Fiber with Triangular Profile

The graded fiber with triangular profile is an interesting case, since it allows for simplified explanations of some interesting properties of the SMS setup.

For simplicity, we assume triangular fiber profile with very large core and with index profile

$$n(x) = n(R) - \frac{\Delta}{a} |x| = n(R) - \frac{NA^2}{(2na)} |x| \quad x < a$$

$$n(x) = n(R) - \Delta \quad x \geq a \quad (4)$$

where x is distance measured from the core axis and a is fiber core radius (i.e., $x = r - R$).

The simplified description of triangular fiber profile represented above can be also used as a rough estimation for parabolic fiber with large core. By inserting typical values for standard telecommunication fiber with $2a = 62.5 \mu\text{m}$, $\Delta = 0.0285$ and $n_{\text{max}} = 1.5$ in (8) we get the critical macrobend radius R_T where propagation of fundamental mode becomes impossible

$$R_T = 1.6 \text{ mm.}$$

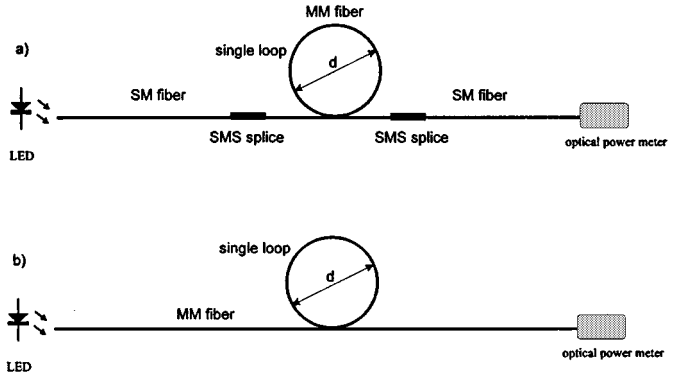


Fig. 6. Experimental setup.

The practical meaning of this estimate is presented in experimental section. Additionally, we assume $x \ll R$ and we rewrite expression (1) in

$$\beta(x) = \frac{R}{R+x} \beta(R) \approx \beta(R) - \frac{x}{R} \beta(R). \quad (5)$$

The effective refractive index of the mode is then expressed as

$$n_{\text{eff}}(x) = \frac{\beta(x)}{k_0} \approx n_{\text{eff}}(R) - \frac{x}{R} n_{\text{eff}}(R). \quad (6)$$

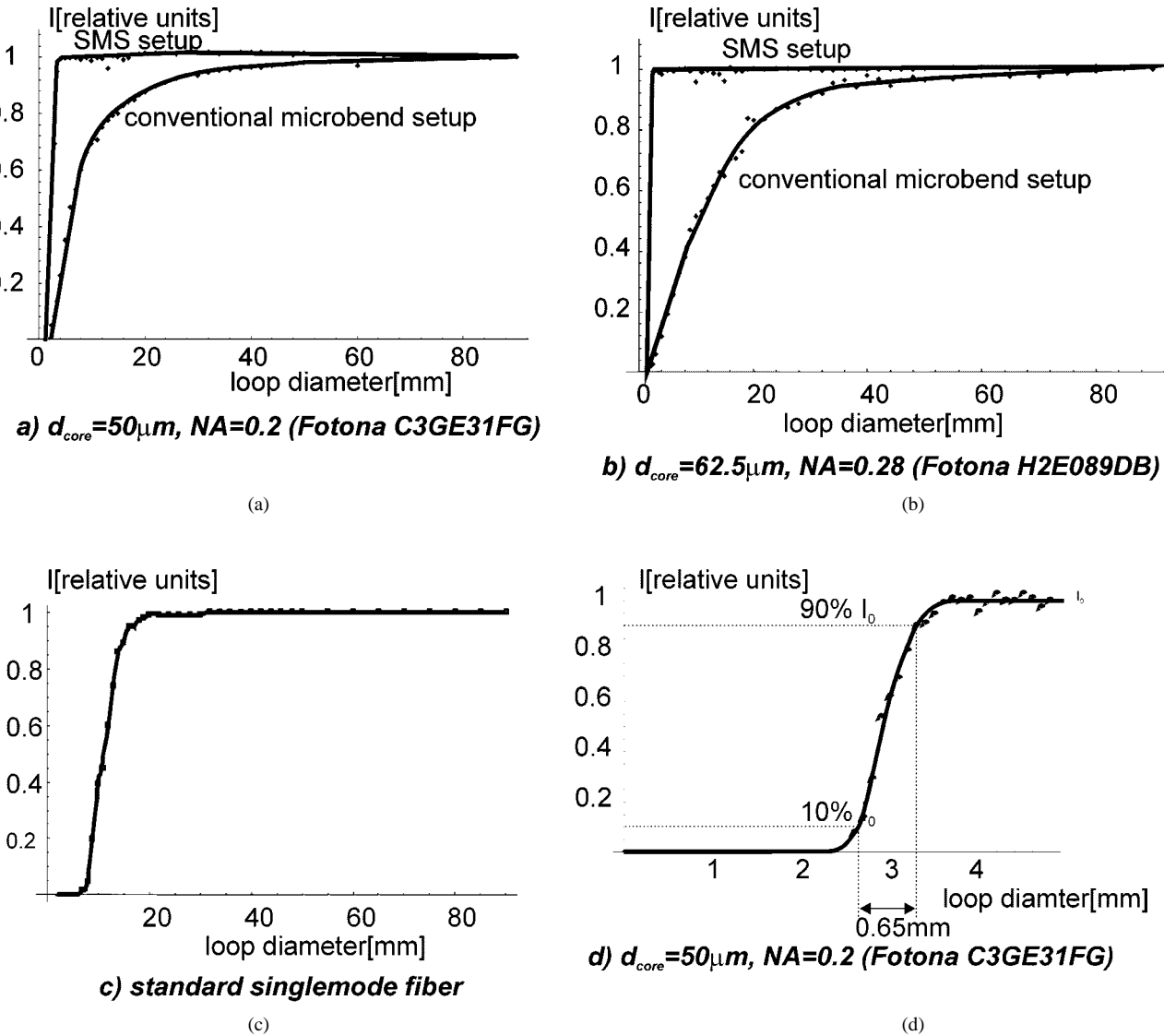


Fig. 7. Output intensity as function of single loop diameter introduced to: (a) and (b) standard multimode fibers—characteristics for SMS and conventional (fully mode excited) setup; (c) standard singlemode fiber; (d) represents the same fiber as in figure (a) in SMS setup, except the “step characteristics” around R_c was investigated in detail. Around the R_c the optical power drops from 90% of initial power to 10% when loop diameter is changed only for 650 μm .

The bent triangular fiber is loss-less, if there is no third region (i.e. evanescent region is infinite). Therefore, for large values of x , the following condition must be fulfilled:

$$n_{\text{eff}}(x) > n(x). \quad (7)$$

From (4), (6), (7), and assuming $n_{\text{eff}}(R) \approx n(R) = n_{\text{max}}$, we get an approximate condition for loss less propagation of fundamental mode in large, triangular core graded fiber:

$$R_T > \frac{a n(R)}{\Delta}. \quad (8)$$

In a hypothetical infinite core, bent triangular fiber there is no finite size evanescent region. The evanescent field is either infinite or it does not exist (i.e., this happens when condition (8) is not fulfilled). This suggests that an infinite core fiber hypothetically exhibit very sharp “step” like bend loss characteristics (the

transition from guided to unguided regime is abrupt when R is decreased below R_T). For a finite core fiber there are always three regions (including finite evanescent region). However in case of sufficiently large core one might intuitively expect that the bend-loss characteristic is similar to infinite core case (i.e., abrupt, “step” like characteristics near critical radius R_T can be expected).

D. Macrobends and Mode Coupling Loss

The remaining question is, do severe macrobends cause coupling of fundamental mode to higher order modes in graded index fiber and thereby loss similar to microbend loss? Since all modes obey equation (1), phase constants of all modes change equally (at least in first approximation) on departing from the axis of the bent fiber—Fig. 5, i.e., curves representing $\beta(r)/k_0$ of different modes never intersect. This keeps the modes (about) equally spaced in β space. Additionally, modes in typical graded telecommunication fibers are about equally spaced in β space with typical beat length of the neighborhood modes of 1.1–1.2

TABLE I
MEASURED $2R_c$ AND CALCULATED $2R_T$
CRITICAL DIAMETERS

Fibre	$2R_c$	$2R_T$
Fotona 50/125 NA=0.2	$2.95\text{mm} \pm 0.1\text{mm}$	5.4mm
Fotona 62.5/125 NA=0.28	$<2\text{mm}^*$	3.2mm
FJC 50/125 NA=0.2	$3.2\text{mm} \pm 0.1\text{mm}$	5.4mm
FJC 62.5/125 NA=0.275	$<2\text{mm}^*$	3.75mm
Alcatel 50/125 NA=0.2	$3.10\text{mm} \pm 0.1\text{mm}$	5.4mm
Alcatel 62.5/125 NA=0.28	$<2\text{mm}^*$	3.6mm
Fotona 50/125 NA=0.15	$7.6\text{mm} \pm 0.1\text{mm}$	9.9mm
Fotona 34/125 NA=0.143	$5.9\text{mm} \pm 0.1\text{mm}$	7.1mm

* The fibre broke before we reached single loop diameter where 3dB of power was lost.

mm, which is comparable to very good HB fiber). This means that neighborhood modes remain well separated in β space. Even in strongly bent fiber there will be low mode coupling.

E. Mode Selectivity of Macrobends

Description given above explains low loss SMS propagation in bent fibers. Higher order modes behave differently. The value of propagation constant decreases with increasing mode number and evanescent field extends further into the cladding. The situation is depicted in Fig. 5. From Fig. 5 one can see that at certain bend radius R the highest order modes of the fiber become completely radiative, while the lowest order modes exhibit negligible loss.

A macrobend therefore behaves as low-pass modal filter. Due to the fast decaying nature of evanescent field, one can expect quite significant modal selectivity of the macrobend loops. This suggests that one can significantly reduce macrobend sensitivity of conventional multimode fiber by restricted modal launch.

III. EXPERIMENTAL RESULTS

A. Experimental Investigation of Macrobend Sensitivity of the SMS Structure

The basic experimental setup is shown in Fig. 6. A single loop was introduced to the multimode fiber in an SMS setup and the output optical power was observed as function of loop diameter d [see Fig. 6(a)]. The single-mode lead fibers were sufficiently long (i.e., few meters) in order to strip cladding modes. The setup shown in 6(b) was used to demonstrate the difference between SMS and conventional setup. In all experiments we used 1300 nm LED source ($\Delta\lambda \approx 60$ nm).

The experimental results for some typical standard telecommunication fibers are shown in Fig. 7. For the SMS setup a very sharp, “step” like characteristic with very small critical macrobend bend radius is typical, while in the case of conventional fiber we observe a gradual loss of optical power as the diameter of the macrobend loop decreases. In fully mode launched setup, significant loss of optical power can be observed at relatively large diameters of the macrobend loop. For comparison we added typical SMF macrobend loss characteristics [Fig. 7(c)]. We also define a new experimental parameter R_c , as diameter of single macrobend loop where optical power drops for 3 dB from initial intensity in straight fiber. Table I summarize R_c and R_T of the tested fibers. The R_c is about 3 mm and less

than 2 mm for standard 50- and 62.5- μm telecommunication fibers, respectively! This is in reasonable agreement with expression (8), especially if we take into account that in bent fiber the photo-elastic effect contributes to bend loss reduction (i.e., effective radius of bent fiber is about 25–30% larger than actual physical radius [6]).

In addition to standard fibers a set of nonstandard fibers with reduced core were produced for SMS structure evaluation. The experimental results for those fibers are shown in Fig. 8 and partially in Table I. Fibers in Figs. 8(b) and (c) and are basically standard graded index fibers, but the outside layers of the core were removed. These two fibers and standard telecommunication fibers exhibit about the same microbend sensitivity in the SMS set-up (i.e., $\Delta\beta$ of neighborhood modes is about the same for all fibers in Figs. 7(a), (b), and 8(b), (c)), while macrobend sensitivity decreases as core size increases—this is graphically presented in Fig. 9.

Fig. 8(a) shows the typical macrobend response for a low NA graded index fiber. Similarly to standard NA fibers one sees a reasonably sharp step characteristics in SMS and gradually decaying power for conventional multimode setup. In both cases the macrobend sensitivity is increased as expected due the reduced NA. The critical diameter for SMS setup is around 7.5 mm.

Fig. 10 presents typical 50 μm ($2R_c = 2.95$ mm) multimode fiber bend loss in SMS setup versus arc length for three different bend radii near R_c . In all three cases the loss is linearly proportional to arc length on a log scale, indicating the presence of only pure bend loss mechanisms [4], [5]. Fig. 10 also demonstrates tremendous differences in bend loss near R_c . At a bend diameter of 3.6 mm the bend loss coefficient is only 0.0035 dB/mm, while at 2.6 mm (only 27% change in diameter) the bend loss increases to 0.4 dB/mm (i.e., more than 100 \times in dB scale).

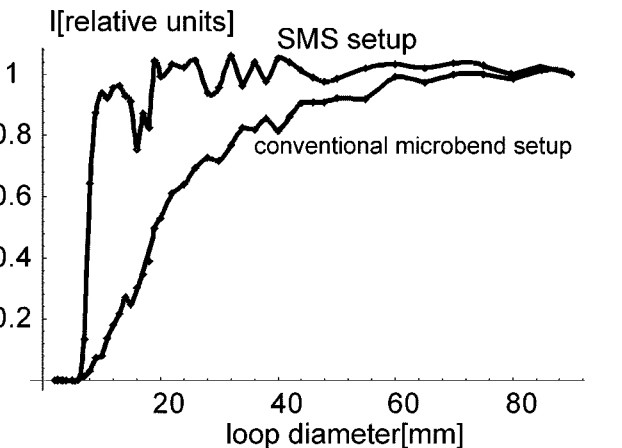
B. The Experimental Investigation of Modal Filtering Properties of Macrobends Introduced to Graded Fiber

Previously, we anticipated that macrobends act as spatial modal filters.

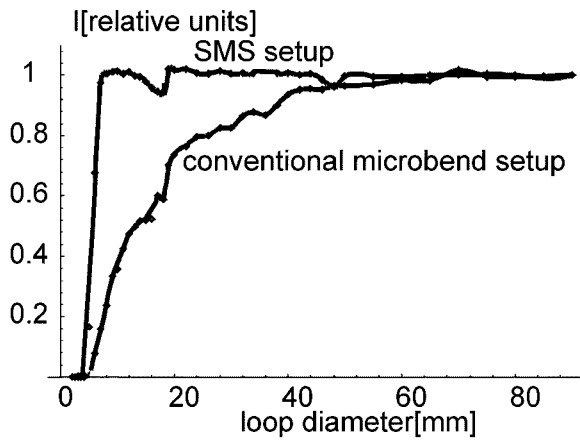
The experimental setup used in this investigation is shown in Fig. 11. The SMF was aligned with the multimode fiber and after that both fibers were offset by a distance y . If y is the offset between single-mode and multimode fiber axes one launches modes with propagation constants that are about in the range of

$$\beta_{\text{launched}}(y) = k_0 n_1 \sqrt{1 - 2\Delta \left(\frac{y}{a}\right)^2} \quad \text{for } y < a. \quad (9)$$

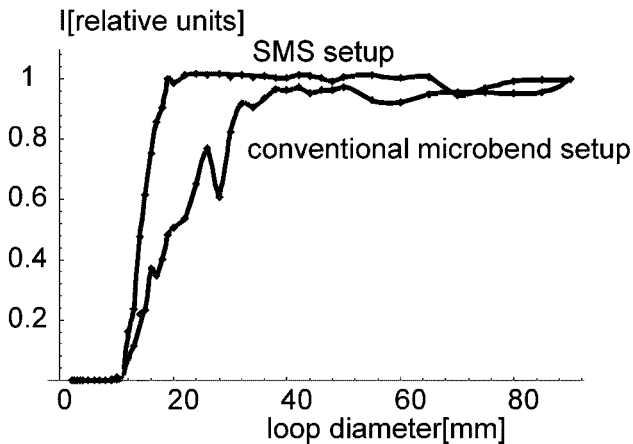
The launch is more selective for small offset y due to the better overlap integral (i.e., when offset is 0 we launch mostly the fundamental mode). Finally, we observed light intensity at the output of the multimode fiber at different fiber offsets and different loop diameters. The results are summarized in Figs. 12 and 13. Fig. 13 represents critical macrobend radius as a function of effective refractive index of the mode dived by refractive index of the core (i.e., $\beta/k_0 n_1$). Data for Fig. 13 was extracted from Fig. 12. Expression (9) was used to (approximately) determine the effective refractive index of the mode from the displacement y of the fibers.

a) $d_{core} = 50.6 \mu m$, $NA = 0.15$ (Fotona G3HE09BA)

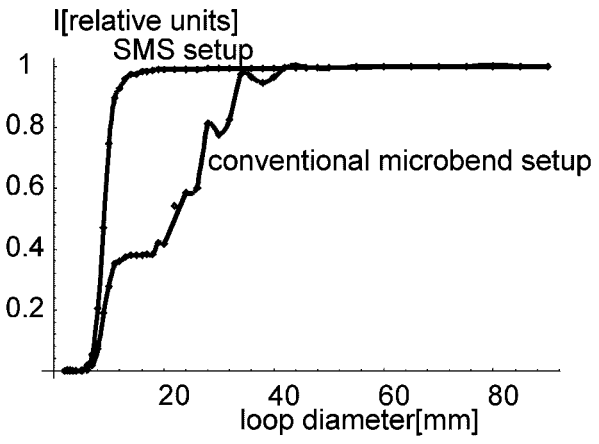
(a)

b) $d_{core} = 33 \mu m$, $\Delta = 0.007$ (Fotona H3JS03BA)

(b)

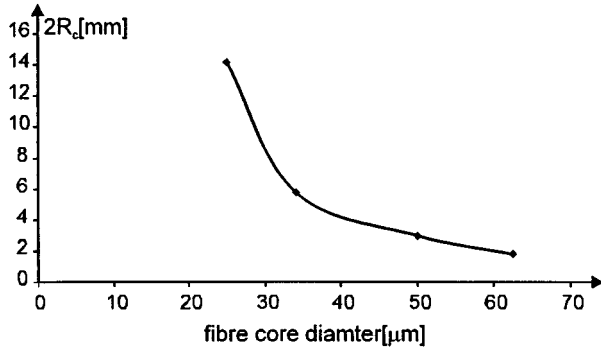
c) $d_{core} = 25 \mu m$, $\Delta = 0.0038$ (Fotona H3IS04BC)

(c)

d) $d_{core} = 16 \mu m$, $\Delta = 0.005$ (Fotona H3IS04BC)

(d)

Fig. 8. Output intensity as function of single loop diameter introduced to some nonstandard multimode fibers for SMS setup and conventional (fully multimode).

Fig. 9. Critical diameter $2R_c$ versus fiber core diameter in case of fibers with same refractive index gradient (all fibers have about the same spacing of neighborhood modes in β space and therefore about the same microbend sensitivity).

From Figs. 12 and 13, one can see that macrobends act as very effective spatial low-pass mode filters. The macrobend sensitivity of the multimode fiber system can be therefore significantly reduced by selective modal launch (the best results are

achieved in the SMS set-up. However any restricted launch of lower order modes can significantly reduce the macrobend loss.

C. Application of the SMS Structure in Macrobend Fiber Optics Sensors

The SMS structure can be configured as very simple, small and effective displacement (and/or force) sensor or fiber optic attenuator. In order to achieve the best sensitivity and linear response characteristics the bend diameter in vicinity of $2R_c$ should be varied in response to an environmental change.

A simple example of displacement sensor is shown in Fig. 14. Fiber is initially spooled to the radius $2R$ and glued to flat deformation plates. When plates are vertically displaced (i.e. in x direction) the fiber spool is deformed into an ellipse and local radius at the sides of spool decreases, which increases macrobend loss. The actual choice of the initial radius depends on desired sensitivity, initial loss, and the application of the sensor. It should be determined experimentally. The displacement sensitivity ($\Delta I / \Delta x$) also depends on number of loops. The higher

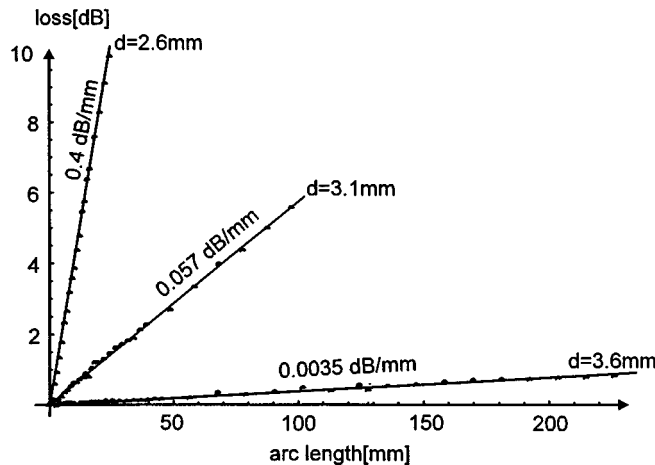


Fig. 10. Bend loss versus arc length for different bend diameters d . For given diameters there is no evidence of significant transition loss.

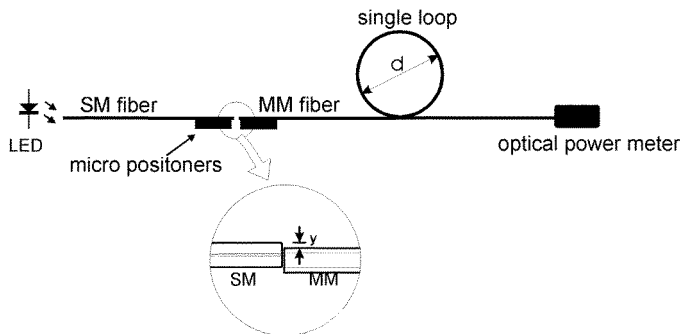


Fig. 11. Experimental setup for determination of macrobend mode filtering properties.

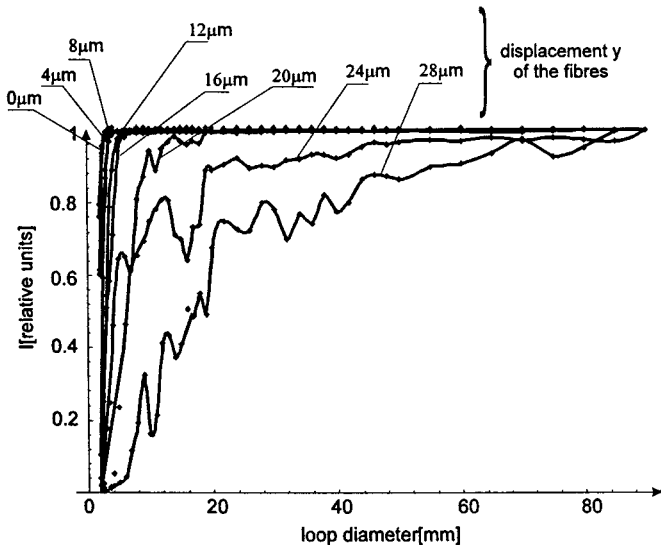


Fig. 12. Light intensity at the output of the multimode fiber as function of launch offset y and diameter of the single macrobend loop introduced to the fiber.

the number of loops the higher is displacement sensitivity (i.e., each loop, when distorted removes the same fraction of initial optical power), but the higher number of loops also increases initial loss. The situation is reversed in case of force measurements (i.e. when self-rigidity of the fiber spool is used as an

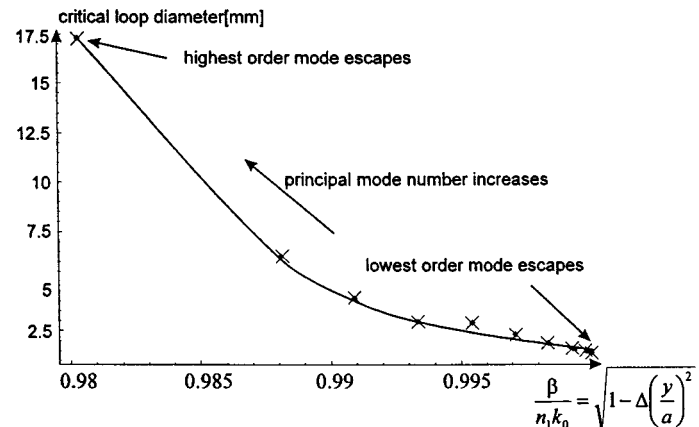


Fig. 13. The critical macrobend radii (i.e. radii where 3 dB of optical power is lost out of the multimode fiber) as $\beta/k_0 n_1$ of the mode. This figure was obtained from Fig. 12 and effective refractive index was estimated from displacement y and (9).

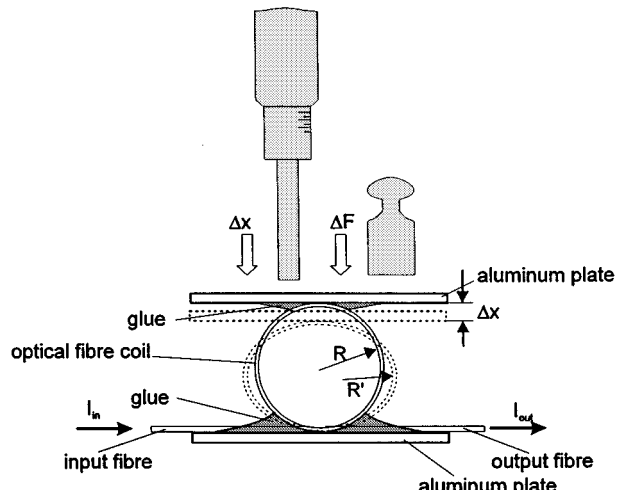


Fig. 14. An example of SMS based macrobend sensor for force and displacement and force sensing.

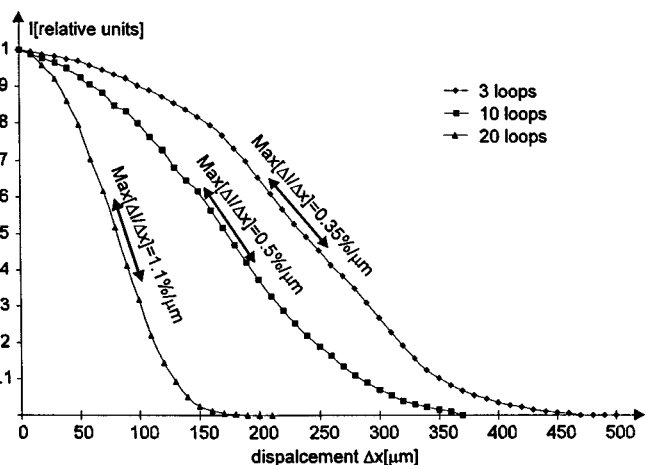


Fig. 15. Experimentally measured sensor response for displacement x . A fiber coil was made of 3, 10, and 20 loops of standard 50- μm fiber. The inner radius of the coil was 3.8 mm. The maximal achieved sensitivity $\Delta I/\Delta x$ was 0.35%/ μm , 0.5%/ μm , and 1.1%/ μm , respectively.

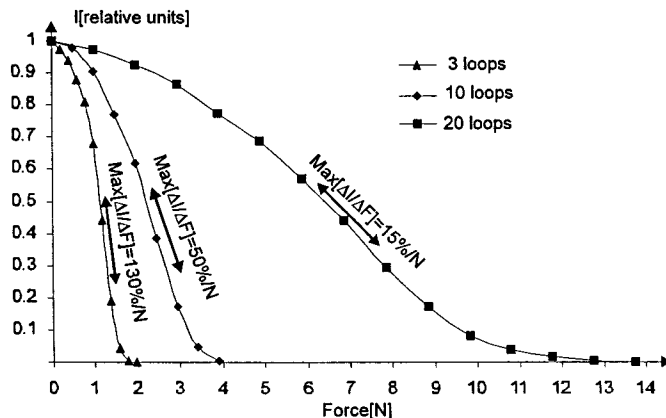


Fig. 16. Experimentally measured sensor response for force F . A fiber coil was made of 3, 10, and 20 loops of standard 50- μm fiber. The inner radius of the coil was 3.8 mm. The maximal achieved sensitivity $\Delta I/\Delta F$ was 130%/N, 50%/N, and 15%/N, respectively.

elastic element). Larger number of loops means more rigid spool and therefore the sensitivity to force in general decreases. Typical response characteristics are shown in Figs. 15 and 16. Fig. 15 shows relative intensity I versus displacement x and Fig. 16 shows relative intensity I versus force F . We used 50- μm standard graded index fiber with critical diameter $2R_c = 2.95$ mm. The initial diameter of the sensor spool $2R$ was 3.8 mm. We tested three sensors each consisting of fiber spool with different number of loops. The initial loss (SM to SM transition) of three loop sensor was 0.89 dB, 2.2 dB for ten loop sensor and 2.9 dB for 20 loop sensor. We achieved maximum $\Delta I/\Delta x$ sensitivity in the range of 1.1%/ μm for the 20 loop sensor. The maximum achieved $\Delta I/\Delta F$ sensitivity was about 130%/N for the three loop sensor. It is obvious that increasing number of loops increases $\Delta I/\Delta x$ sensitivity and reduces $\Delta I/\Delta F$ sensitivity.

Though the higher $\Delta I/\Delta x$ sensitivity can be achieved with 62.5- μm fibers (smaller R_c) the preferred solution for sensing applications are mostly 50- μm fiber. This is predominantly due to small R_c of the 62.5- μm fibers, which results in high mechanical stress (62.5- μm fiber tended to break by itself after certain time when we spooled it diameter close to $2R_c$ —this problem could be probably eliminated by the use of metal coated fiber and thermal annealing process).

IV. CONCLUSION

A novel structure was proposed for obtaining sharp bends in dielectric waveguides without significant increase in loss. The major property of the structure is step-like macrobend charac-

teristics. The macrobend loss remains low for bend diameters larger than a certain critical bend diameter of the fiber, but when the diameter of the bend is reduced below this critical value macrobend loss rises abruptly. The critical diameter is in the range of few millimeters for standard graded index fibers. The structure, called SMS, uses selective launch and filtering of the fundamental mode in graded index multimode fiber. An approximate quantitative theoretical model and an extensive experimental investigation of the proposed structure were presented.

Simple, compact and relatively sensitive macrobend sensors based on the SMS structure were demonstrated. The basis for the macrobend sensor construction is step like characteristics of the proposed structure. We practically demonstrated sensitivities in the range of $\Delta I/\Delta x = 1.1\%/\mu\text{m}$ and $\Delta I/\Delta F = 130\%/\text{N}$ and even higher sensitivities are possible by proper mechanical construction of the sensor element. The same setup can be used as a well-behaved, simple and compact fiber optic attenuator.

REFERENCES

- [1] D. Marcuse, "Curvature loss formula for optical fibers," *J. Opt. Soc. Amer.*, vol. 66, no. 3, pp. 216–220, 1976.
- [2] D. Marcuse, "Field deformation and loss caused by curvature of optical fibers," *J. Opt. Soc. Amer.*, vol. 66, no. 4, pp. 311–320, 1976.
- [3] J. A. Buck, *Fundamentals of Optical Fibers*, Wiley Series in Pure and Applied Optics. New York: Wiley, 1995.
- [4] R. C. Gauthier and C. Ross, "Theoretical and experimental consideration for single-mode fiber optic bend-type sensors," *Appl. Opt.*, vol. 36, no. 25, pp. 6264–6273, 1997.
- [5] W. A. Gambling, H. Matsumura, C. M. Ragdale, and R. A. Sammut, "Measurement of radiation loss in curved singlemode fibers," *Microwaves, Opt. Acoust.*, vol. 2, no. 4, pp. 134–140, 1978.
- [6] A. B. Sharma, A.-H. Al-Ani, and S. J. Halme, "Constant-curvature loss in monomode fibers: An experimental investigation," *Appl. Opt.*, vol. 23, no. 19, pp. 3297–3301, 1984.
- [7] A. J. Harris and P. F. Castle, "Bend loss measurements on high numerical aperture single-mode fibers as a function of wavelength and bend radius," *J. Lightwave Technol.*, vol. 4, pp. 34–40, Jan. 1986.
- [8] E. G. Neumann and W. Richter, "Sharp bends with low losses in dielectric optical waveguides," *Appl. Opt.*, vol. 22, no. 7, pp. 1016–1022, 1983.
- [9] D. Donalgić and B. Culshaw, "Microbend sensor structure for use in distributed and quasi distributed sensor systems based on selective launching and filtering of the modes in graded index multimode fiber," *J. Lightwave Technol.*, vol. 17, pp. 1856–1869, Oct. 1999.
- [10] D. Marcuse, "Gaussian approximation of the fundamental modes of graded-index fibers," *J. Opt. Soc. Amer.*, vol. 68, no. 1, 1978.

Denis Donalagić, photograph and biography not available at the time of publication.

Brian Culshaw, photograph and biography not available at the time of publication.